THE JOURNAL OF BIOLOGICAL CHEMISTRY
Vol. 278, No. 49, Issue of December 5, pp. 48981–48990, 2003

Printed in U.S.A.

The N-terminal Zinc Binding Domain of ClpX Is a Dimerization Domain That Modulates the Chaperone Function*

Received for publication, July 18, 2003, and in revised form, August 21, 2003
Published, JBC Papers in Press, August 23, 2003, DOI 10.1074/jbc.M307825200

Urszula A. Wojtyra‡, Guillaume Thibault‡§, Ashleigh Tuite, and Walid A. Houry¶

From the Department of Biochemistry, Medical Sciences Building, 1 King's College Circle, University of Toronto, Toronto, Ontario M5S 1A8, Canada

Clp ATPases are unique chaperones that promote protein unfolding and subsequent degradation by proteases. The mechanism by which this occurs is poorly understood. Here we demonstrate that the N-terminal domain of ClpX is a C4-type zinc binding domain (ZBD) involved in substrate recognition. ZBD forms a very stable dimer that is essential for promoting the degradation of some typical ClpXP substrates such as λO and MuA but not GFP-SsrA. Furthermore, experiments indicate that ZBD contains a primary binding site for the λO substrate and for the cofactor SspB. Removal of ZBD from the ClpX sequence renders the ATPase activity of ClpX largely insensitive to the presence of ClpP, substrates, or the SspB cofactor. All these results indicate that ZBD plays an important role in the ClpX mechanism of function and that ATP binding and/or hydrolysis drives a conformational change in ClpX involving ZBD.

Clp ATPases are a unique group of ATP-dependent chaperones associated with the disassembly of protein complexes (1). They are members of the AAA family of proteins, which are ATPases associated with a variety of cellular activities. The key feature of this family is a highly conserved AAA module of about 230 amino acids that is present in one or more copies in each protein. Each module can typically be divided into two subdomains: one $\alpha\beta$ and one all α (2). In the $\alpha\beta$ subdomain, there is a conserved Walker A motif, involved in binding the phosphate of ATP, and a Walker B motif, involved in metal binding and ATP catalysis (3). The unifying structural feature of these AAA proteins is the arrangement of the subunits into ring-shaped hexameric or heptameric complexes.

The main Clp ATPases in the *Escherichia coli* cytoplasm are ClpA, ClpB, ClpX, and HslU. They function to unfold proteins or to disaggregate protein aggregates. They all have N-terminal domains followed by AAA modules, except for HslU, which has an insertion in the AAA module that is thought to correspond to the N-terminal domains in the other Clps (4). Both ClpA and ClpB have two AAA modules, whereas ClpX and HslU have only one, which is homologous to the second AAA module in ClpA and ClpB (3). ClpA and ClpX form hexameric complexes that can associate with ClpP (5), a serine protease consisting of two rings with 7-fold symmetry (6). Several ClpXP and ClpAP substrates are known (reviewed in Ref. 1). ClpA substrates include RepA, HemA, N-end rule proteins, and ClpA itself. Known ClpX substrates include λO, MuA, Mu repressor, UmuD′, σ^S, and Phd. Some of these proteins, such as λO and RepA, are recognized by the chaperones mainly through their N termini, whereas others, like MuA and Mu repressor, seem to be recognized mainly through their C termini. More recently, a proteomics approach revealed more than 50 potential ClpXP substrates in *E. coli* (7). Analysis of these substrates revealed three C-terminal ClpX recognition consensus sequences and two such N-terminal sequences.

Both ClpXP and ClpAP have been implicated in the degradation of C-terminally SsrA-tagged proteins (8). The SsrA tag, which has a very hydrophobic sequence of 11 amino acids, is cotranslationally added to the C terminus of stalled nascent chains (9). In addition, ClpA and ClpX have been shown to bind to adaptor proteins that affect their function (10–12). SspB enhances the degradation efficiency of C-terminally tagged SsrA proteins by ClpXP (13, 14). It has been proposed that an SspB dimer binds to two GFP-SsrA molecules and that this complex subsequently binds to the ClpX hexamer (12).

A number of elegant studies have demonstrated the ability of ClpX and ClpA to unfold native proteins (15–18). Experiments have suggested that unfolding, translocation, and degradation take place in a unidirectional manner starting from the attachment point of the degradation tag (19, 20). The importance of the N-terminal domain of Clp ATPases in these processes has been rather enigmatic. The N terminus of ClpB from *Thermus thermophilus* has been shown not to be essential for chaperone activity *in vitro* (21), and ClpB from the cyanobacterium *Synechococcus* sp. strain PCC 7942 with the N terminus deleted was able to restore bacterial thermotolerance *in vivo* (22). On the other hand, *E. coli* ClpB lacking its N terminus was shown to be either inactive (23) or active (24) as a chaperone *in vitro* depending on the assay being used. ClpA deleted of the N terminus can mediate the ClpP-dependent degradation of SsrA-tagged substrates (11, 25, 26) but not RepA (25). Similarly, the N terminus of ClpX is not required for the degradation of GFP-SsrA by ClpXP but is required for the degradation of λO (26).

The importance of the N-terminal domain of ClpX is evident from its conservation across all sequenced genomes. The domain is present in almost all known *clpX* sequences (Table I). Here we demonstrate that the N-terminal domain of ClpX is a C4-type zinc binding domain (ZBD)[1] that forms a very stable

* This work was supported in part by a Canadian Institutes of Health Research grant. The costs of publication of this article were defrayed in part by the payment of page charges. This article must therefore be hereby marked "*advertisement*" in accordance with 18 U.S.C. Section 1734 solely to indicate this fact.

‡ Contributed equally to this work.

§ Supported by a National Sciences and Engineering Council of Canada Postgraduate Scholarships A fellowship.

¶ Canadian Institutes of Health Research New Investigator. To whom correspondence should be addressed. Tel.: 416-946-7141; Fax: 416-978-8548; E-mail: walid.houry@utoronto.ca.

[1] The abbreviations used are: ZBD, zinc binding domain; GFP, green fluorescent protein; MBP, maltose binding protein; PAR, 4-(2-pyridylazo)resorcinol; PMB, p-hydroxymercuribenzoate; ICP-AES, inductively coupled plasma atomic emission spectroscopy; ELISA, enzyme-linked immunosorbent assay; BSA, bovine serum albumin; Ni-NTA, nickel-nitrilotriacetic acid.

TABLE I
Conservation of ClpP and ClpX across different genomes

The *E. coli* ClpP and ClpX protein sequences were used to BLAST against 16 archaeal, 124 bacterial, and 15 eukaryotic completely sequenced genomes in NCBI (July, 2003 version). All ClpX protein sequences were aligned and checked for the presence of the zinc binding motif ($CX_2CX_{18\text{-}40}CX_2C$), where *X* is any amino acid, as well as for the presence of the ClpP binding motif IGF (37). "No" refers to the absence of the gene if BLAST and tBLASTn programs did not provide a hit (E-value cutoff was e^{-30}).

		ClpP	ClpX		
		Present	Present	ZBD	IGF
Archaebacteria	16 complete genomes	No	No		
Bacteria	118 genomes	Yes	Yes	Yes	Yes
	Mollicutes, six complete genomes	No	No		
Eukaryotes					
Fungi	*Neurospora crassa*	No	Yes	No	Yes
	Saccharomyces cerevisiae	No	Yes	No	No
	Schizosaccharomyces pombe	No	No		
	Encephalitozoon cuniculi	No	No		
Plant	*Arabidopsis thaliana*	Yes	Yes (3)	Yes (2), No (1)	Yes (3)
	Oryza sativa	Yes	Yes	Yes	Yes
Animal	*Caenorhabditis elegans*	Yes	Yes	Yes	Yes
	Anopheles gambiae	Yes	Yes	Yes	Yes
	Drosophila melanogaster	Yes	Yes	Yes	Yes
	Homo sapiens	Yes	Yes	Yes	Yes
	Mus musculus	Yes	Yes	Yes	Yes
	Rattus norvegicus	Yes	Yes	Yes	Yes
Cryptophyta	*Guillardia theta* NUCLEOMORPH	Yes	No		
Alveolata	*Plasmodium falciparum*	Yes	No		

constitutive dimer, which is necessary for binding of λO and SspB to ClpX. In addition, we show that, unlike the full-length chaperone, the presence of ClpP, substrates, or cofactors does not significantly affect the ATPase activity of ClpX lacking the zinc binding domain.

EXPERIMENTAL PROCEDURES

Subcloning and Mutagenesis—All proteins were expressed from the pProEX HTb vector (Invitrogen) except for MBP-ZBD[1–60], which was expressed from pMAL C2 vector (New England Biolabs). Point mutations were introduced using the QuikChange system (Stratagene) according to manufacturer's protocol. All constructs were verified by DNA sequencing.

pET9aClpP overexpressing untagged ClpP was a gift from Dr. John Flanagan (Brookhaven National Laboratory). pRLM266 overexpressing λO protein was a gift from Dr. Roger McMacken (Johns Hopkins University). pMK951 overexpressing MuA protein was a gift from Dr. George Chaconas (University of Western Ontario).

Protein Purification and Peptide Synthesis—All tagged proteins were purified according to the manufacturer's protocols, and, if required, the tag was removed using tobacco etch virus protease. ClpP (27), λO (28), and MuA (29) were purified according to published protocols. Protein concentrations were determined using either the Bradford assay or the 5,5′-dithiobis(nitrobenzoic acid) assay to measure cysteine content. The SsrA peptide was synthesized using Fmoc (*N*-(9-fluorenyl)methoxycarbonyl) solid phase chemistry.

Analysis of ZBD Zinc Content—Zinc content was analyzed either by inductively coupled plasma atomic emission spectroscopy (ICP-AES), using a PerkinElmer Life Sciences Optima 3000 spectrometer or by a colorimetric assay. For ICP-AES, protein samples were dialyzed against two changes of Buffer A (50 mM Hepes, pH 7.8, and 150 mM NaCl) containing 10–20 mg/ml Chelex resin (Bio-Rad). The emission of 19 metals was monitored. In the colorimetric assay, ZBD was diluted to 5 μM in Buffer B (25 mM TrisHCl, pH 8, and 150 mM NaCl) containing 100 μM 4-(2-pyridylazo)resorcinol (PAR) at room temperature and then *p*-hydroxymercuribenzoate (PMB) was titrated into the solution. A sample was removed after each addition to monitor formation of $PAR_2{\cdot}Zn^{+2}$ at 500 nm. The average of the Zn^{+2} concentration, determined from a standard curve, released after four molar equivalents of PMB was divided by the protein concentration in the assay to determine the moles of Zn^{+2} metal bound per mole of protein monomer.

Mu Phage Assay—Mu phage particles were isolated and purified from HM8305 F′ Mu*cts62 E. coli* strain, according to published protocols (30). The strain was a gift from Dr. George Chaconas (University of Western Ontario). Mu phage plaque formation at 37 °C in MC4100 *clpX*::Kan^R strain transformed with different ClpX mutants was measured. The strain was a gift from Ariane Toussaint (Université Libre de Bruxelles). All experiments were carried out in triplicate.

Measurement of GFP-SsrA Expression and Stability in Vivo—E. coli strains MC4100 and MC4100 *clpX*::Kan^R were transformed with pGFP or pGFP-SsrA ($Chloramphenicol^R$) (31), and the Δ*clpX* strains were subsequently transformed with pProEX HTb (Amp^R) plasmid encoding *clpX* or *clpX*Δ*ZBD* genes. Cultures were grown at 37 °C in LB medium with appropriate antibiotic selection until A_{600} of ~0.4, and the expression of GFP and GFP-SsrA was induced using 0.2% arabinose. Samples were taken at 20, 40, and 60 min post-induction and diluted to an A_{600} of ~0.3 using Buffer C (25 mM TrisHCl, pH 7.5, and 150 mM NaCl). Fluorescence was measured by setting excitation at 395 nm and monitoring emission from 410–600 nm. The emission was normalized to the peak at 456 nm, which is dependent on the density of the cells.

Coexpression of H_6-ZBD[1–60] and ClpX—The plasmids pET28b and pET3a expressing H_6-ZBD and ClpX, respectively, were transformed into BL21(DE3) cells, and the coexpression of the two proteins was induced with isopropyl-1-thio-β-D-galactopyranoside. ClpX was also expressed alone as a control. Cells from 50 ml of culture were lysed by sonication in Buffer D (25 mM TrisHCl, pH 7.5, 500 mM NaCl, 10% glycerol, 5 mM β-mercaptoethanol, and 10 mM imidazole) with 1 mg/ml lysozyme after 20 min of incubation on ice. Purification was carried out according to the manufacturer's protocol. Bound proteins were eluted with Buffer D plus 250 mM imidazole. Proteins were then separated on SDS-PAGE.

Cross-linking of ZBD[1–60]—Cross-linking was carried out in Buffer E (25 mM Hepes, pH 7.9, 150 mM NaCl, 100 μM $ZnCl_2$, and 1 mM dithiothreitol) using glutaraldehyde at a final concentration of 0.05% and a final protein concentration of 1 μM. Samples were removed at different time points, and the reaction was quenched by adding TrisHCl, pH 8, to a final concentration of 0.5 M.

Sedimentation Equilibrium Analysis of ZBD[1–60]—Sedimentation equilibrium experiments and analysis were performed at the Analytical Centrifugation Facility at the Ontario Cancer Institute (Toronto). ZBD[1–60] was exchanged into Buffer F [25 mM Hepes, pH 7.9, 150 mM NaCl, and 2 mM tri(2-carboxyethyl)phosphine] and diluted to concentrations of 100, 166, and 233 μM. Experiments were performed at four different speeds at 20 °C.

Circular Dichroism of ZBD—CD measurements were obtained using an AVIV Circular Dichroism spectrometer Model 62ADS or a Jasco J-810. Proteins were diluted into Buffer G (25 mM TrisHCl, pH 8, 150 mM NaCl, 100 μM $ZnCl_2$, and 1 mM dithiothreitol).

Fitting the Denaturation Curves—To analyze the data from thermal and chemical denaturation experiments, a model where the native ZBD dimer (N_2) unfolds directly to two unfolded monomers (U) was used. Analysis was carried out according to Bowie and Sauer (32); however, a global fit to the Gibbs-Helmholtz equation, shown in Equation 1, was

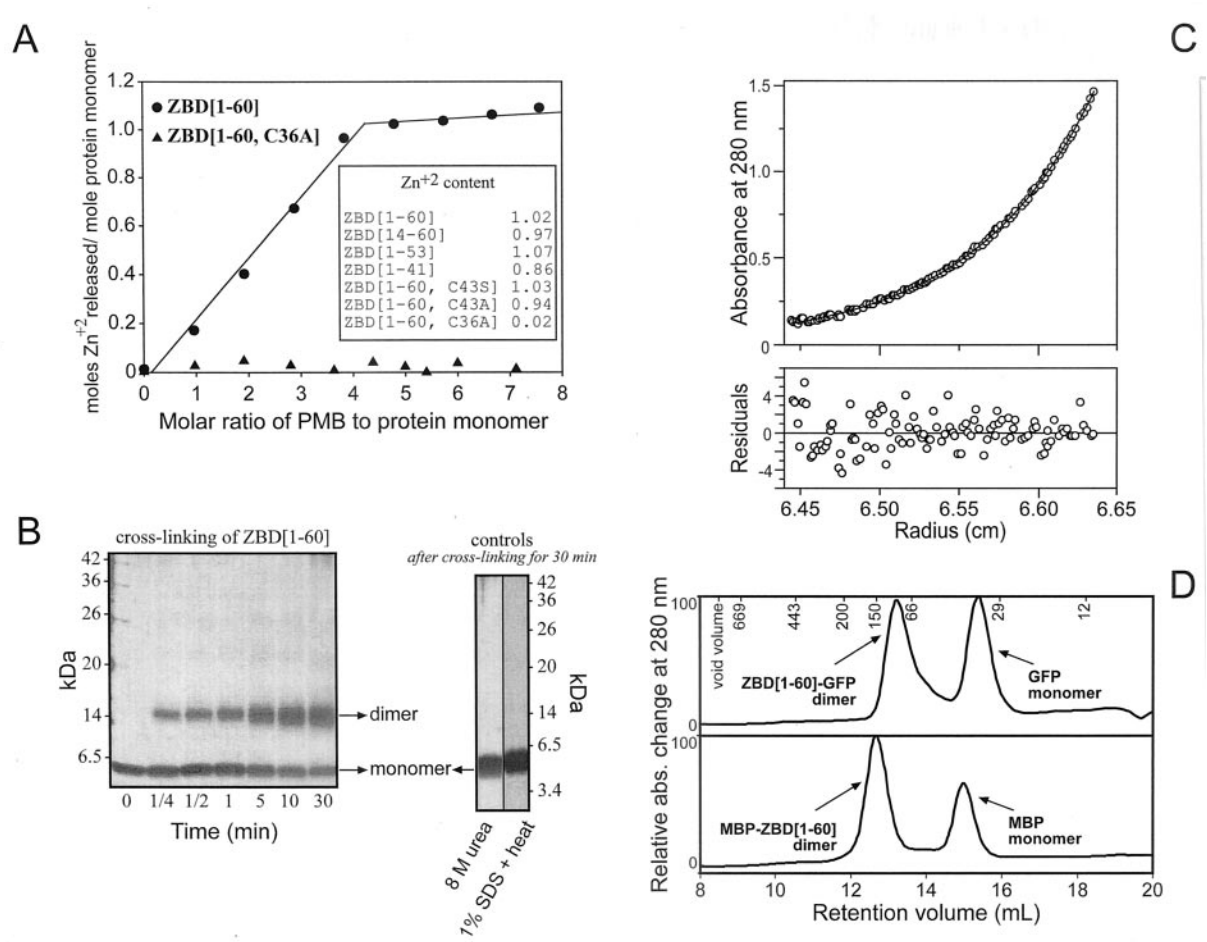

FIG. 1. **Zinc binding and dimerization of ZBD.** *A*, the release of Zn^{+2} from ZBD[1–60] (●) or ZBD[1–60, C36A] (▲) was monitored by absorbance at 500 nm to follow the formation of $(PAR)_2{\cdot}Zn^{+2}$ complex upon addition of PMB. The complete release of Zn^{+2} from ZBD[1–60] required 4 moles of PMB to one mole of ZBD[1–60]. The measured Zn^{+2} content of other ZBD mutants are listed in the table. *B*, ZBD[1–60] was incubated at 1 μM in Buffer E in the presence of 0.05% glutaraldehyde. At indicated *time points*, the reaction was quenched by the addition of TrisHCl to 0.5 M, and samples were separated on SDS-PAGE and visualized by silver staining. As control, the protein was either heat-denatured in 1% SDS or denatured in 8 M urea and subjected to cross-linking as above; only the 30-min time point is shown. *C*, the *upper panel* shows the sedimentation equilibrium ultracentrifugation data for ZBD[1–60] at 166 μM. *Points* shown were collected at 33,000 rpm and 20 °C. The *solid line* is the theoretical fit to the data using a single species function of ZBD[1–60] dimer. The *lower panel* displays residual deviations from the theoretical fit. *D*, a mixture of GFP (27 kDa) and ZBD[1–60]-GFP (34 kDa) or of MBP (43 kDa) and MBP-ZBD[1–60] (50 kDa) was loaded onto a calibrated Superdex 200 gel filtration column equilibrated in Buffer G. Molecular mass markers (kDa) are shown on the top *x* axis. The proteins migrated at the following positions: 35, 100, 40, 120 kDa, respectively. Because the ZBD[1–60] dimer alone migrates as a 28-kDa protein, ZBD[1–60]-GFP and MBP-ZBD[1–60] migrate at the expected molecular masses of dimers (28 + 2 × 35 and 2 × 40 + 28, respectively).

done to obtain T_m, $\Delta H(T_m)$, and ΔC_p, where T_m is the temperature at which $K_U = [U]^2/[N_2] = 1$.

$$\Delta G_U = \Delta H(T_m)\left(1 - \frac{T}{T_m}\right) + \Delta C_p\left[T - T\ln\left(\frac{T}{T_m}\right) - T_m\right] \quad \text{(Eq. 1)}$$

Degradation Assays—Assays were typically carried out by preincubating a degradation mixture consisting of 1.5 units of creatine kinase, 16 mM creatine phosphate, 3 mM ATP, 4 μM substrate protein, 1.2 μM ClpP in Buffer H (25 mM Hepes, 5 mM $MgCl_2$, 5 mM KCl, 0.03% Tween 20, and 10% glycerol) at 37 °C for 3 min. Subsequently, 1 μM ClpX or ClpX mutant was added to the reaction, and the incubation was continued at 37 °C. All concentrations are those of monomers. Samples were taken at the indicated time points, and the degradation was stopped by addition of 4× Laemmli buffer and boiling. Proteins were then separated on SDS-PAGE, and the intensities of the protein bands (IPB) were quantified using ImageQuant 5.0. The initial rate (V_0) was determined from the slope of the plot of ln(IPB) *versus* time for the first 5 min of the reaction. Degradation of GFP-SsrA was also monitored by fluorescence using a Fluorolog spectrofluorometer (Jobin Yvon) with the excitation wavelength set at 395 nm and the emission wavelength set at 509 nm. For the GFP-SsrA competition assays, SsrA peptide, λO, MuA, or SspB were preincubated with the degradation mixture prior to the addition of ClpX.

ELISA Assay—The wells of a 96-well plate were coated with λO, MuA, GFP-SsrA, or BSA (100 μl, 20 μg/ml) in 20 mM Na_2CO_3, pH 9, for 1 h at 37 °C. The wells were then washed with Buffer I (25 mM TrisHCl, pH 7.5, 150 mM NaCl, and 0.1% Tween 20) and incubated with 200 μl of 5% milk protein in Buffer I for an additional hour at 37 °C. The wells were then washed with Buffer J (25 mM Hepes, pH 7.5, 150 mM KCl, 25 mM NaCl, 10 mM $MgCl_2$, 2.5% glycerol, 0.1 mM EDTA, and 0.1% Tween 20) plus 1 mM dithiothreitol and incubated with increasing amounts of ZBD[1–60] for 1 h (total volume 100 μl). This step and all subsequent steps were performed at room temperature. Wells were washed with Buffer J (200 μl, three times), incubated with 100 μl of a 1:3000 dilution of anti-ClpX serum for 1 h, and washed and then horseradish peroxidase-conjugated Protein A (1:10,000 dilution, 100 μl) in Buffer J was added to the wells and incubated for 1 h. The wells were washed, and 100 μl of 3,3′,5,5′-tetramethylbenzidine liquid substrate (T0440; Sigma) was added. The reaction was allowed to proceed for 30 min, and the absorbance was measured at 650 nm using a SPECTRAmax 340PC plate reader (Molecular Devices).

ATPase Activity Using NADH—ATPase activity of ClpX was measured using a coupled assay (33). Assays were typically carried out by preincubating 1.0 μM ClpX or ClpX mutant, 0.2 mM NADH, 3.0 mM phosphoenolpyruvate, 4.7 units of pyruvate kinase, and 7.4 units of lactate dehydrogenase in Buffer H at 37 °C for 3 min. 1.2 μM ClpP, 4

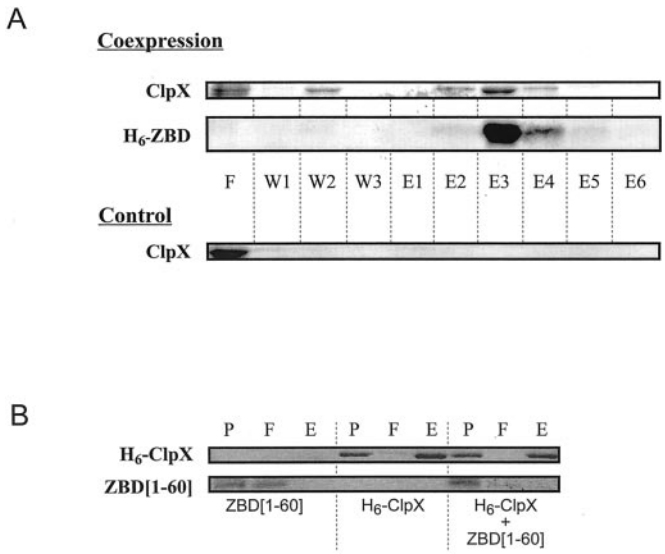

FIG. 2. **ZBD is a dimer in context of the full-length chaperone.** *A*, untagged ClpX was either coexpressed with H_6-ZBD[1–60] (*top two panels*) or expressed alone (*bottom panel*), and the lysates were then passed over Ni-NTA resin. The flow-through was collected, and afterward the beads were washed with 10 mM imidazole. Bound material was subsequently eluted with 250 mM imidazole. *B*, purified untagged ZBD[1–60], purified H_6-ClpX, or a mixture containing 10 μM ZBD[1–60] and 10 μM H_6-ClpX was passed over Ni-NTA column. *P*, *F*, *W*, and *E* refer to protein prior to loading onto the column, flow-through, washes, and elutions, respectively.

μM GFP-SsrA, 4 μM λO, or 0.33 μM SspB were included as indicated. Subsequently, 5 mM ATP was added to the reaction, and the change in absorbance at 340 nm was measured for 20 min at 37 °C. The rate of ADP formation was calculated assuming a 1:1 correspondence between NADH oxidation and ATP regeneration and an extinction coefficient of 6230 M^{-1} cm^{-1} (33). The assay was repeated at least three times.

RESULTS

The N Terminus of ClpX Is a Dimer Containing a C4-type Zinc Binding Motif—Purified ClpX (10 μg in 140 μl) was subjected to limited proteolysis using sub-stoichiometric amounts of trypsin. The resulting peptides were analyzed by matrix-assisted laser desorption ionization time-of-flight mass spectrometry. At very low trypsin quantities (0.1 ng), a 7-kDa peptide that mapped to the N-terminal 60 amino acids of ClpX was detected (numbering according to Swiss-Prot P33138). This region appeared to be very stable and was not degraded with higher protease quantities. Our results are generally consistent with earlier observations made by Singh *et al.* (26). Subsequently, the N terminus of ClpX was cloned and purified, and its ability to bind Zn^{+2} was characterized using ICP-AES and a colorimetric assay (Fig. 1*A*). Both techniques clearly demonstrated that the N terminus of ClpX spanning residues 1–60 bound Zn^{+2} in a ratio of one Zn^{+2} ion per protein monomer. We call this domain ZBD[1–60] for zinc binding domain of ClpX spanning residues 1 to 60. Only the first four cysteines (Cys-14, Cys-17, Cys-36, and Cys-39) are involved in chelating the Zn^{+2}, because mutants lacking the fifth cysteine (Cys-43) were still able to bind Zn^{+2} in one to one molar ratio, whereas the C36A mutant resulted in the formation of a destabilized domain that did not contain Zn^{+2} (Fig. 1*A*). These results, as well as previous observations (34), clearly suggest that the highly conserved $CX_2CX_{18-40}CX_2C$ motif in ZBD of ClpX is a C4-type zinc finger.

ZBD[1–60] migrated as a 28-kDa protein on a gel filtration column (not shown). This is much larger than a monomer, because the predicted molecular mass of ZBD[1–60] is 7.046 kDa. Consequently, the oligomeric state of ZBD[1–60] was further investigated using several techniques. In an initial approach, chemical cross-linking was performed using glutaraldehyde. It was found that a cross-linked dimer could be detected in as little as 15 s, and higher oligomers were not detected even after 30 min (Fig. 1*B*). This oligomerization was judged to be specific at the protein concentration used (1 μM), because denaturation of ZBD[1–60] either by chemical or heat treatment (Fig. 1*B*) yielded no detectable dimeric species even after 30 min. ZBD[1–60] was further characterized by sedimentation equilibrium analytical ultracentrifugation at higher concentrations (100, 166, and 233 μM). The data was best fit to a single species with an apparent molecular mass of 14.94 kDa (Fig. 1*C*). This value is very close to the expected molecular mass of a dimer. The dimerization of ZBD[1–60] is not mediated by Cys-43, because ZBD[1–41] also formed a dimer as determined by gel filtration (not shown). ZBD[1–53], which has the domain boundaries identified by Singh *et al.* (26), also migrated as a dimer.

Furthermore, ZBD was able to force the dimerization of known monomers. Two fusion proteins, ZBD[1–60]-GFP (N-terminal fusion with green fluorescent protein) and MBP-ZBD[1–60] (C-terminal fusion with maltose binding protein), migrated as dimers when examined by size exclusion chromatography (Fig. 1*D*). Both GFP and MBP migrated as monomers. These experiments, together with the cross-linking and ultracentrifugation data, clearly demonstrate that the N-terminal domain of ClpX is not a monomer as published previously (26), but rather forms a stable dimer.

To demonstrate that this domain exists as a dimer in the context of the full-length chaperone, ClpX and His-tagged ZBD[1–60] were coexpressed and purified on a Ni-NTA column. ClpX co-purified on Ni-NTA only when coexpressed with His-tagged ZBD, whereas it did not bind to the resin non-specifically in the absence of H_6-ZBD[1–60] (Fig. 2*A*). However, when purified, untagged ZBD[1–60], which is already dimeric, was mixed with purified His-tagged ClpX, which forms mixed oligomers, and then passed over the Ni-NTA column, no interaction between the two proteins was observed (Fig. 2*B*). H_6-ClpX bound specifically to the column, whereas untagged ZBD[1–60] did not bind to the column. Similarly, Singh *et al.* (26) had shown that the N-terminal domain of ClpX does not interact with the rest of the chaperone as determined by gel filtration. Hence, in the coexpression experiment, untagged ClpX must be interacting with His-tagged ZBD[1–60] through the dimerization of newly synthesized H_6-ZBD[1–60] with the N-terminal domains of newly synthesized ClpX. This surprising observation of the dimerization of the ClpX N terminus leads us to propose that the hexameric ClpX could possibly function as a trimer-of-dimers.

Stability of the ZBD Dimer—CD spectra of ZBD[1–60] were obtained for the native, denatured, and renatured protein (Fig. 3*A*). The spectrum of the renatured protein overlays perfectly with that of the native protein, indicating that thermal denaturation is completely reversible. Thermally and chemically induced unfolding of ZBD[1–60], as monitored by CD at 220 nm, was reversible and occurred in a cooperative fashion, with a single transition region (Fig. 3, *B* and *C*). The stability of ZBD[1–60] was decreased in the presence of EDTA (Fig. 3*B*) indicating that Zn^{+2} is a structural metal necessary for the stability of this small domain. Furthermore, the denaturation profile exhibited a concentration dependence as expected for a protein oligomer (compare 3 to 30 μM in Fig. 3*B*). This result further establishes ZBD[1–60] as a dimer. The single transition observed upon thermal and chemical denaturation, and the concentration dependence of the denaturation process, all indicate that the dimer is present in the unfolding transition region. The monomer is not populated to a great extent in that

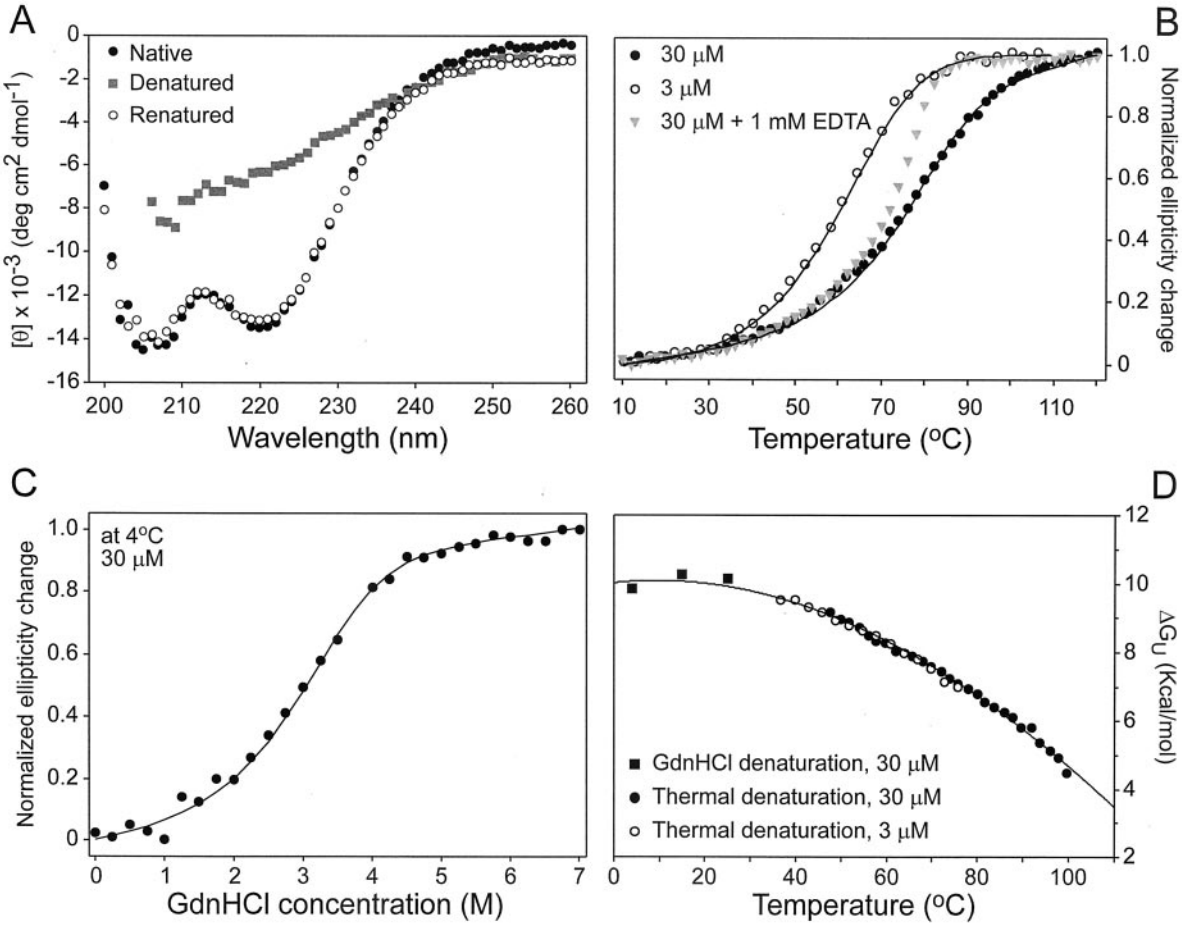

FIG. 3. **Secondary structure and stability of ZBD[1–60].** *A*, the CD spectra of ZBD[1–60], expressed as mean residue ellipticity, at 10 °C (●), 110 °C (*gray squares*), and refolded (○) at 10 °C after denaturation at 110 °C. Protein concentrations in all spectra were 30 μM dissolved in Buffer G. *B*, thermal denaturation of ZBD[1–60] monitored by circular dichroism at 220 nm. Denaturation was performed at protein concentrations of 30 μM (●) and 3 μM (○) in the absence of EDTA and at 30 μM in the presence of 1 mM EDTA (▼). Thermal denaturation was reversible in all cases. Experiments were performed in Buffer G. *Solid lines* represent the theoretical curves obtained from fitting the data in *D* to the Gibbs-Helmholtz equation. *C*, GdnHCl denaturation of ZBD[1–60] at 30 μM and 4 °C in Buffer G monitored by circular dichroism at 220 nm. Denaturation was reversible. *Solid line* represents the theoretical fit to the data assuming a linear dependence of ΔG_U on [GdnHCl] (43), $\Delta G_U = \Delta G_U^{H_2O} - m$[GdnHCl], which gives m = 1.3 Kcal mol^{-1} M^{-1} and $\Delta G_U^{H_2O}$ at 4 °C = 9.85 Kcal mol^{-1}. *D*, unfolding free energy of ZBD[1–60] as a function of temperature. *Circles* represent ΔG_U calculated from the transition zones of the thermal denaturation curves of ZBD[1–60] at 30 μM (●) and 3 μM (○). GdnHCl denaturation was performed at three different temperatures (4, 15, and 25 °C), and the $\Delta G_U^{H_2O}$ (■) were calculated. *Solid line* shows the least squares fit to the Gibbs-Helmholtz equation, which yields ΔC_p = 0.41 Kcal mol^{-1} K^{-1}, T_m = 135 °C, and $\Delta H(T_m)$ = 61.8 Kcal mol^{-1}.

region, because the free energy of unfolding, ΔG_U, in the transition region of the thermal denaturation is the same at the two different concentrations (Fig. 3*D*). Therefore, the denaturation data were fit to a two state model where the native ZBD[1–60] dimer (N_2) unfolds directly to two unfolded monomers (*U*). Based on this model and the fit of the data in Fig. 3*D* to the Gibbs-Helmholtz equation (see "Experimental Procedures"), the thermodynamic parameters for ZBD[1–60] stability at 25 °C were found to be ΔG_U = 9.9 Kcal mol^{-1}, ΔH_U = 16.5 Kcal mol^{-1}, ΔS_U = 22 cal mol^{-1} K^{-1}, and ΔCp = 0.41 Kcal mol^{-1} K^{-1}. These values demonstrate that ZBD[1–60] is a very stable dimer that can withstand thermal stress and is ideally suited to be a domain in a protein involved in heat stress response.

ZBD Is Essential for ClpX Function in Mu Phage Replication—Replicative transposition during the lytic cycle of bacteriophage Mu requires the function of the ClpX chaperone (35). In an *E. coli* strain lacking the chromosomal *clpX* gene, the last step in transposition, which is the remodeling of the MuA transposase complexes, is blocked, because MuA remains bound to DNA as a tetramer (36), and, hence, the formation of plaques is prevented. A *clpX* knockout strain was transformed with plasmids expressing wild-type and mutant versions of the ClpX protein, and the ability to form plaques was assessed (37). It was found that plaque formation in the wild-type strain was comparable with that of the knockout strain expressing wild-type ClpX from a plasmid (Fig. 4*A*). Interestingly, ClpX lacking ZBD[1–60] (ClpXΔZBD) could not support the lytic growth of Mu phage even at high concentrations of phage. The inability to complement the knockout phenotype was observed with ZBD[1–60] alone and with an ATPase deficient mutant, ClpX (K124Q); this mutation in the Walker A motif prevents ATP hydrolysis and renders the chaperone inactive. The expression levels and solubility of ClpX and the different mutants were similar in these cells (not shown).

The Role of ZBD in GFP-SsrA Degradation in Vivo—GFP-SsrA was expressed in wild-type cells, as well as in cells deleted of *clpX* gene expressing ClpX or ClpXΔZBD from a plasmid. After 20, 40, and 60 min of induction of GFP-SsrA, a fluorescence emission scan of the intact cells was obtained. In the *clpX* knockout cells, the peak because of GFP-SsrA fluorescence is evident with peak maximum at 508 nm (Fig. 4*B*, *top right*). This characteristic peak is absent in the wild-type strain or in the *clpX* knockout strains expressing either ClpX or ClpXΔZBD. In all four strains, untagged GFP was expressed to similar extents, and its levels were not reduced by the expression of ClpX (*insets* in Fig. 4*B*). Thus, ClpXΔZBD is active in

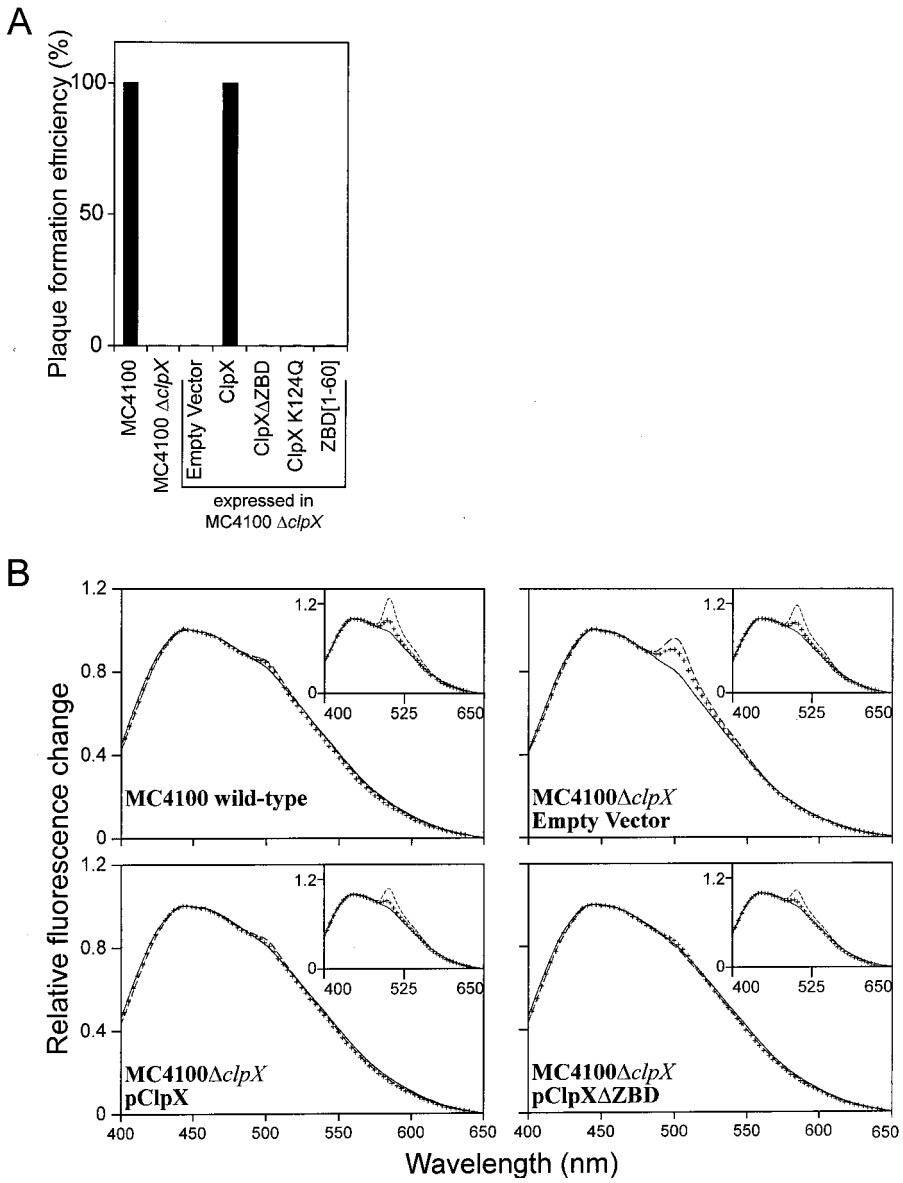

FIG. 4. **The importance of ZBD for ClpX *in vivo* function.** *A*, MC4100 *clpX*::Kan^R was transformed with a pProEX HTb plasmid encoding wild-type ClpX or various mutants. These transformed strains were infected with Mu*cts62* phage at various dilutions. Formed plaques were counted and normalized to the wild-type strain. Each *bar* represents the average of at least three experiments. *B*, the normalized fluorescence emission spectrum of GFP-SsrA present in intact wild-type MC4100 cells (*top left*), or in MC4100 *clpX*::Kan^R cells transformed with empty vector (*top right*), or with pProEX HTb plasmid encoding ClpX (*bottom left*) or ClpXΔZBD (*bottom right*). *Insets* show the fluorescence of untagged GFP in these same strains. In all cases, samples were taken at 20 (*solid line*), 40 (*crosses*), and 60 (*dashed line*) min after induction of GFP or GFP-SsrA using 0.2% arabinose.

degrading GFP-SsrA *in vivo* although it cannot function in disassembling MuA-DNA complexes. Hence, ZBD could be required for binding and/or unfolding of some substrates such as MuA but not GFP-SsrA. This possibility is investigated further.

ZBD Modulates Substrate Degradation by ClpXP—To further investigate the role of ZBD in ClpX function, the degradation reactions of GFP-SsrA, MuA, and λO were carried out at 37 °C in the presence of ClpP, ATP, an ATP regenerating system, and ClpX or ClpXΔZBD (Fig. 5*A*). At different time points, samples were withdrawn from the degradation assay, boiled in Laemmli buffer, and separated on SDS-PAGE. The degradation of GFP-SsrA was also monitored by fluorescence (Fig. 6). These experiments revealed several unexpected results.

The ClpP-dependent degradation of GFP-SsrA can be mediated by ClpX lacking ZBD as determined by quantifying the bands on the gel or by fluorescence (Fig. 5*A*, *right panel* and Fig. 6, *E–H*, 0 μM *curves*). This is in agreement with our *in vivo* observations (Fig. 4*B*), as well as with the observations of Singh *et al.* (26), who used enzymatically truncated ClpX. This indicates that the primary binding site for the SsrA tag is in the AAA domain of ClpX and not in the ZBD. However, the degradation of GFP-SsrA by ClpXΔZBD/ClpP was 33% less efficient than by ClpXP; this could reflect that ZBD further enhances the unfoldase activity of ClpX because of the presence of a secondary binding site for GFP-SsrA on ZBD. It should be noted that none of the ClpX constructs were able to degrade GFP-SsrA(DD) or GFP-SsrA in the presence of ADP or absence of ATP (data not shown).

On the other hand, ZBD seems to be absolutely essential for the binding and/or unfolding of λO, because ClpXΔZBD/ClpP was not able to degrade λO (Fig. 5*A*, *right panel*). This has been observed before with ClpX in which the first four cysteines involved in chelating Zn^{+2} were mutated to serines (34) and with ClpX treated with limiting amounts of V8 protease to remove the first 54 amino acids (26). Furthermore, ClpXΔZBD was six times less efficient than ClpX in mediating the degradation of MuA (Fig. 5*A*). This result is consistent with the inability of ClpXΔZBD to promote Mu phage replication (Fig. 4*A*). Hence, λO and MuA seem to represent a class of ClpX substrates that, unlike GFP-SsrA, requires the full-length chaperone to be efficiently degraded.

To demonstrate that ZBD is directly involved in substrate binding, ELISA analysis was performed (Fig. 5*B*). GFP-SsrA, MuA, and λO, as well as the nonspecific protein BSA, were bound to the ELISA wells. ZBD[1–60] was added to the wells at

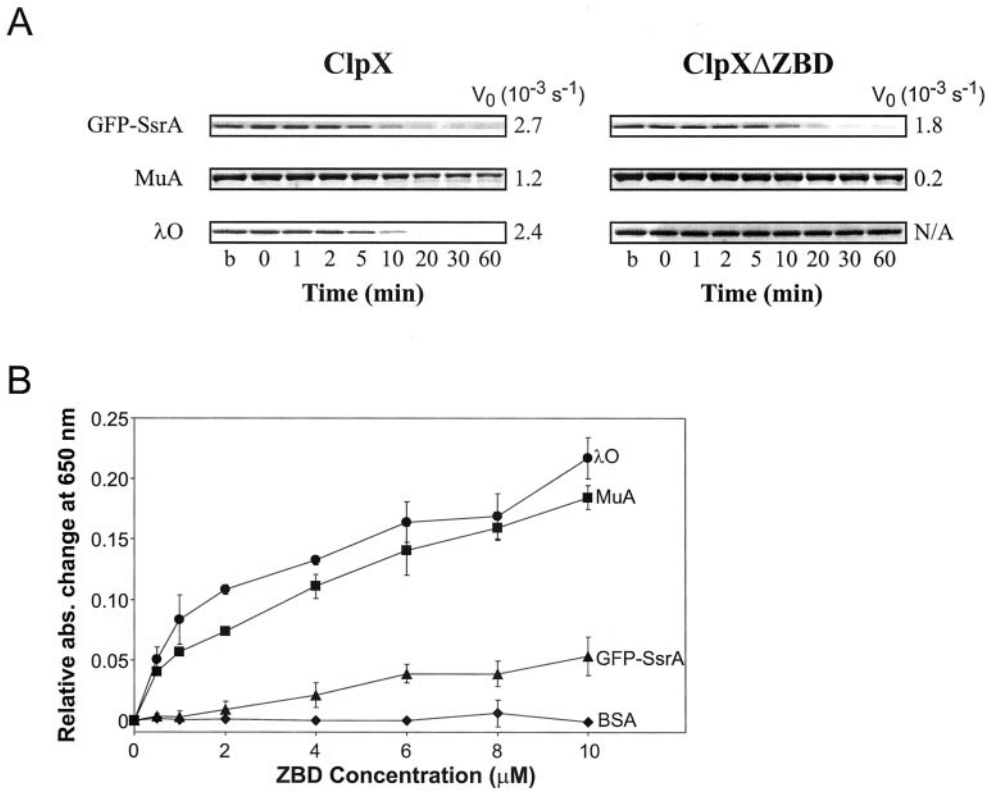

FIG. 5. **Role of ZBD in substrate degradation and binding.** *A*, the degradation of GFP-SsrA, MuA, and λO (each at 4 μM) by ClpXP (*left panel*) or ClpXΔZBD/ClpP (*right panel*) (each at 1 μM) was monitored by SDS-PAGE. Aliquots were removed from the degradation mixture at the indicated *time points*. The chaperone was the last component added to the reaction mixture. *b* refers to before addition of the chaperone. V_0 is the initial rate of substrate degradation (see "Experimental Procedures"). *B*, ELISA assays of the binding of ZBD[1–60] to λO, MuA, GFP-SsrA, and BSA. Data points are the average of three experiments.

increasing concentrations. The amount of bound ZBD[1–60] was detected by first incubating with rabbit anti-ClpX antibodies, followed by incubating with Protein A conjugated to horseradish peroxidase. As can be seen in Fig. 5*B*, ZBD[1–60] bound with similar affinity to λO and MuA but did not interact significantly with GFP-SsrA or BSA. Thus, ClpX contains at least two different binding sites; one is present in the ZBD and is required for binding λO and MuA, and one is within the AAA domain and is essential for binding GFP-SsrA.

To further characterize the substrate binding sites in ClpX, the degradation of GFP-SsrA was performed in the presence of different concentrations of λO, MuA, SsrA peptide, or the cofactor SspB. Each competition assay included ClpP, ATP, an ATP regenerating system, ClpX, or ClpXΔZBD, and the degradation of GFP-SsrA was monitored by fluorescence (Fig. 6). λO, MuA, and the SsrA peptide competed in a concentration-dependent manner for the ClpX-mediated degradation of GFP-SsrA (Fig. 6, *A–C*), whereas SspB enhanced the degradation of GFP-SsrA as expected (Fig. 6*D*) (13). However, for ClpXΔZBD, only the SsrA peptide was able to significantly compete for GFP-SsrA degradation (Fig. 6*G*), further proving that the ZBD is not required for SsrA binding or recognition and that the binding of the SsrA tag occurs in the AAA domain of ClpX. On the other hand, the presence of 50 μM λO, which is at 12.5 times excess over GFP-SsrA, was insufficient to slow down the GFP-SsrA degradation by ClpXΔZBD (Fig. 6*E*). Similar curves were obtained if λO was added 2 min after the start of the reaction (not shown). Hence, ZBD seems to be essential for binding λO. It should be noted that λO at 2 μM was able to slow the degradation by ClpXP of 4 μM GFP-SsrA (Fig. 6*A*) indicating that the full-length chaperone has higher affinity for λO than GFP-SsrA. MuA was also able to compete with GFP-SsrA but much more weakly in the case of ClpXΔZBD as compared with ClpX (Fig. 6, *F versus B*). This suggests that ZBD in ClpX significantly increases the binding affinity of MuA to the chaperone.

The presence of as little as 0.05 μM of the cofactor SspB increased GFP-SsrA degradation by ClpXP (1 μM), and the degradation rate of GFP-SsrA was saturated between 0.33 and 10 μM SspB (Fig. 6*D*). On the other hand, SspB slowed down, rather than enhanced, the degradation of GFP-SsrA by ClpXΔZBD/ClpP (Fig. 6*H*). Hence, the ZBD is essential for the enhancing activity of SspB, which is probably because of the direct binding between SspB and ZBD. For the case of ClpXΔZBD, SspB would directly bind the SsrA tag of GFP-SsrA (12, 14) but would not be able to transfer the substrate to the chaperone because of the absence of ZBD. Therefore, the presence of SspB would protect GFP-SsrA from degradation by ClpXΔZBD/ClpP as observed (Fig. 6*H*). This effect is not seen *in vivo* in Fig. 4*B*, probably because the levels of SspB are much lower than those of overexpressed ClpXΔZBD. Because both SspB and λO require the ZBD for binding to ClpX, it is likely that both proteins bind at the same site(s) or at very close site(s) on ZBD considering the small size of this domain.

ZBD Modulates the ATPase Activity of ClpX—The ATPase activity of ClpX can be stimulated by substrates (38) but is inhibited by ClpP (39). Under the experimental conditions used, the ATPase activity of ClpX alone was 273 pmol min^{-1} μg^{-1} (Fig. 7), which is similar to previously published results (38). The addition of ClpP in the absence of substrates or cofactor lowered the ATPase activity to 218 pmol min^{-1} μg^{-1}. In the absence of ClpP, the ATPase activity of ClpX increased upon addition of 4 μM λO, GFP-SsrA, or GFP-SsrA with 0.33 μM SspB to 944, 574, and 1160 pmol min^{-1} μg^{-1}, respectively (Fig.

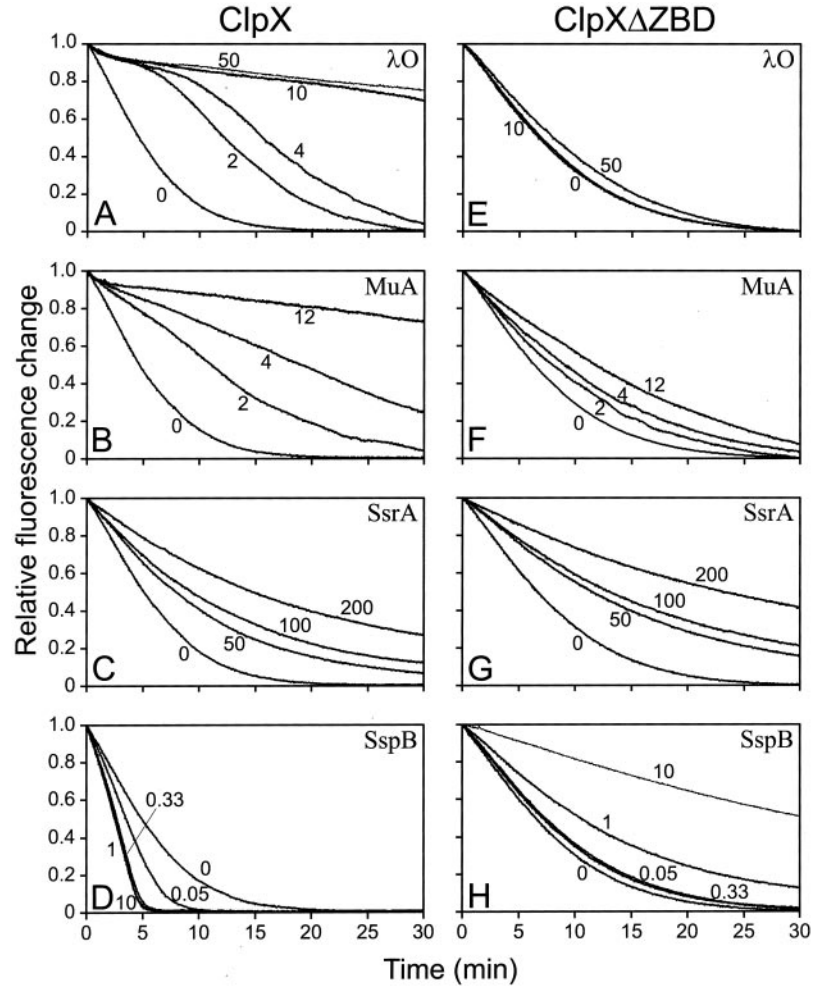

FIG. 6. **The effect of added substrates and cofactors on GFP-SsrA degradation by ClpXP or ClpXΔZBD/ClpP.** The degradation of GFP-SsrA (4 μM) by ClpXP (*A–D*) or ClpXΔZBD/ClpP (*E–H*) (each at 1 μM) was carried out in the presence of exogenous λO (0, 2, 4, 10, and 50 μM), MuA (0, 2, 4, and 12 μM), SsrA (0, 50, 100, and 200 μM), or SspB (0, 0.05, 0.33, 1, and 10 μM). The concentration of the added substrate or cofactor is indicated in μM near the corresponding degradation curve.

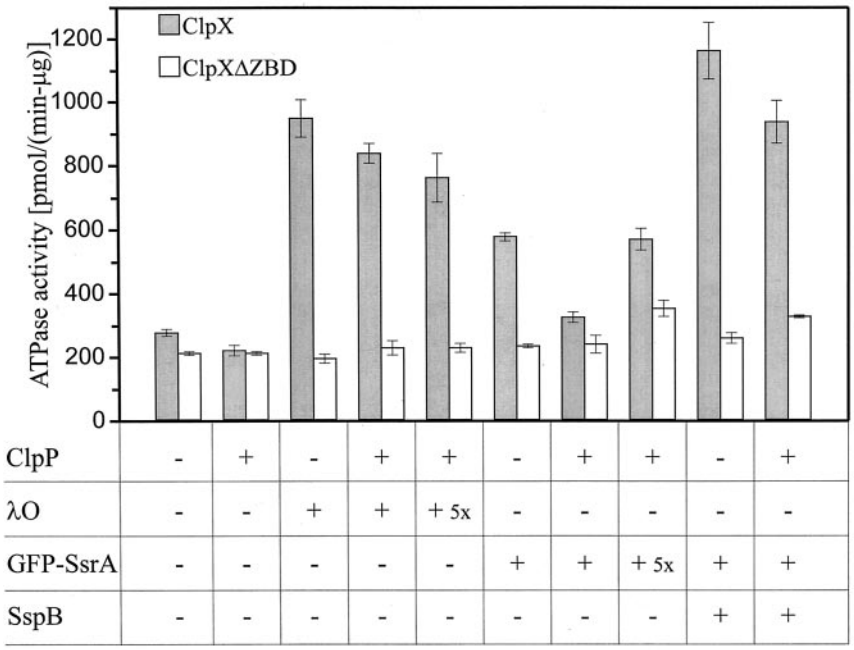

FIG. 7. **Role of ZBD in modulating the ATPase activity of ClpX.** ATPase activity of ClpX (*gray bars*) or of ClpXΔZBD (*empty bars*) (both at 1 μM) was measured in the absence (−) or presence (+) of ClpP (1 μM), λO (4 μM), GFP-SsrA (4 μM), and/or SspB (0.33 μM). 5× indicates the addition of 20 μM of λO or GFP-SsrA.

7). The presence of ClpP lowered those ATPase levels to 835, 328, and 932 pmol min^{-1} μg^{-1}, respectively (Fig. 7). Because the K_d for GFP-SsrA binding to ClpX hexamer is estimated to be around 3 μM (18), and because λO binds ClpX tighter than GFP-SsrA (see above), the concentrations of λO and GFP-SsrA were increased to 20 μM (5x) to saturate the binding between the substrates and ClpX in the presence of ClpP. The ATPase activity of ClpX did not change significantly in the presence of increased λO concentration (759 pmol min^{-1} μg^{-1}) possibly indicating that the lower λO concentration was already satu-

rating; however, in the presence of increased GFP-SsrA, the activity increased back to levels similar to those in the absence of ClpP (568 pmol min^{-1} μg^{-1}).

The ATPase activity of ClpXΔZBD alone was 209 pmol min^{-1} μg^{-1} (Fig. 7), which is only slightly lower than that of ClpX. However, the presence of λO, GFP-SsrA, or GFP-SsrA with SspB did not significantly change the ATPase activity of ClpXΔZBD, and the presence of ClpP did not inhibit the ATPase activity. The presence of five times the substrate concentration also did not significantly affect the ATPase activity of ClpXΔZBD. Based on these results, ZBD seems to be required for the stimulation or inhibition of the ClpX ATPase activity. This effect is probably mediated by a conformational change in ClpX involving ZBD.

It is interesting to note that the ATPase activity of ClpXΔZBD and ClpX in the presence of GFP-SsrA and ClpP correlate with the rate of degradation of GFP-SsrA. GFP-SsrA is degraded about one-third slower by ClpXΔZBD/ClpP than by ClpXP (1.8×10^{-3} *versus* 2.7×10^{-3} s^{-1}; see Fig. 5*A*), and the ATPase activity of ClpXΔZBD is about one-third lower than that of ClpX under the same conditions (237 *versus* 323 pmol min^{-1} μg^{-1}; see Fig. 7). However, this correlation does not extend to other substrates such as λO. This could reflect the difference in binding to ClpX by GFP-SsrA and λO.

DISCUSSION

We have demonstrated that the N terminus of ClpX is a constitutive dimer that contains a C4-type zinc binding region. Cross-linking, ultracentrifugation, gel filtration, and thermal melts all support the conclusion that ZBD is a very stable dimer. The ZBD dimer is reminiscent of the pseudo-2-fold symmetry observed in the ClpA and ClpB N termini (2, 40–42), which can be considered a pseudo-dimer. The N-terminal domain of ClpA has also been observed to contain a Zn^{+2} binding site in its first half consisting of two histidines, a glutamine, and a water molecule; however, there is only one Zn^{+2} bound per pseudo-dimer (41).

Pull-down experiments of coexpressed ClpX and ZBD suggest that ZBD is also a dimer in the context of the full-length ClpX chaperone. Hence, ClpX possibly functions as a trimer-of-dimers. On the other hand, the N termini of ClpA and ClpB have been shown to form monomeric domains (25, 42). Based on the ClpA crystal structure, as well as on electron microscopy studies, the N-terminal domains seem to be very flexible and not fixed in one orientation (2). Because the pseudo-dimer domains of ClpA and ClpB are ~150 amino acids, whereas the ZBD monomer of ClpX is less than half that size (60 amino acids), the protein density above the AAA hexamer of ClpA or ClpB is twice as much as that of ClpX. This could indicate that the N-terminal domain movements in ClpA and ClpB are different from those in ClpX; consequently, the ATP-dependent conformational changes that occur in ClpX might be different from those that occur in ClpA or ClpB implying a different mechanism of function.

In vitro and *in vivo* experiments indicate that ZBD is required for ClpX chaperone function for some substrates such as λO and MuA but not GFP-SsrA (Figs. 4–6). λO is a highly positively charged protein, with arginines or lysines constituting 16% of all its residues, resulting in a pI of 9.4. MuA has a similar character; 14.7% of its residues are lysines and arginines, and it has a pI of 8.9. On the other hand, SsrA (AANDENYALAA) is a very hydrophobic tag with a pI of 3.7. In *E. coli* proteins, the average R+K content is about 10% (refer to EBI Proteome analysis). Hence, λO and MuA may be characteristic of a typical substrate for which ClpX requires the function of the ZBD.

Substrates, cofactors, and interacting partners modulate the ATPase activity of ClpX (Fig. 7). Removal of the ZBD essentially abolishes this modulation. It is reasonable to speculate that the ATP-dependent movement of the ZBD causes the stimulation in the ATPase activity of ClpX. This could be either because of the direct binding of substrates and cofactors to ZBD such as that observed for λO and SspB or as a result of as yet unknown secondary effect because of the binding on the AAA domain, as for GFP-SsrA. The ATPase activity of ClpA and ClpB is also affected by the removal of their N-terminal domains (24, 26). In the case of ClpB, the ATPase activity is higher for the chaperone deleted of the N-domain as compared with the full-length chaperone, but the stimulation by substrates is decreased (24). On the other hand, ClpA lacking the N-domain has lower ATPase activity compared with the full-length protein (26). Thus, it appears that the N-terminal domains of the Clp chaperones play an essential role in regulating ATP hydrolysis in the presence of substrates and cofactors, reflecting an ATP-dependent conformational change involving these domains. Mapping out those conformational changes will be critical to understanding the unfoldase activity of this group of proteins.

Acknowledgments—We thank Brian Cox for help with mass spectrometry, Alan Davidson for the use of his CD instrument, Charlie Deber for use of his peptide synthesizer, Deborah Zamble for help in carrying out the ICP-AES experiments, George Chaconas for help in the Mu phage assay, Ipein Chua, Tanya Cordeiro, Khadija Mahmood, and Jamie Snider for help in cloning some of the constructs, and other members of the Houry laboratory for critical discussions.

REFERENCES

1. Hoskins, J. R., Sharma, S., Sathyanarayana, B. K., and Wickner, S. (2002) *Adv. Protein Chem.* **59,** 413–429
2. Guo, F., Maurizi, M. R., Esser, L., and Xia, D. (2002) *J. Biol. Chem.* **277,** 46743–46752
3. Schirmer, E. C., Glover, J. R., Singer, M. A., and Lindquist, S. (1996) *Trends Biochem. Sci.* **21,** 289–296
4. Bochtler, M., Hartmann, C., Song, H. K., Bourenkov, G. P., Bartunik, H. D., and Huber, R. (2000) *Nature* **403,** 800–805
5. Grimaud, R., Kessel, M., Beuron, F., Steven, A. C., and Maurizi, M. R. (1998) *J. Biol. Chem.* **273,** 12476–12481
6. Wang, J., Hartling, J. A., and Flanagan, J. M. (1997) *Cell* **91,** 447–456
7. Flynn, J. M., Neher, S. B., Kim, Y. I., Sauer, R. T., and Baker, T. A. (2003) *Mol. Cell* **11,** 671–683
8. Gottesman, S., Roche, E., Zhou, Y., and Sauer, R. T. (1998) *Genes Dev.* **12,** 1338–1347
9. Keiler, K. C., Waller, P. R., and Sauer, R. T. (1996) *Science* **271,** 990–993
10. Zhou, Y., Gottesman, S., Hoskins, J. R., Maurizi, M. R., and Wickner, S. (2001) *Genes Dev.* **15,** 627–637
11. Dougan, D. A., Reid, B. G., Horwich, A. L., and Bukau, B. (2002) *Mol. Cell* **9,** 673–683
12. Wah, D. A., Levchenko, I., Baker, T. A., and Sauer, R. T. (2002) *Chem. Biol.* **9,** 1237–1245
13. Levchenko, I., Seidel, M., Sauer, R. T., and Baker, T. A. (2000) *Science* **289,** 2354–2356
14. Flynn, J. M., Levchenko, I., Seidel, M., Wickner, S. H., Sauer, R. T., and Baker, T. A. (2001) *Proc. Natl. Acad. Sci. U. S. A.* **98,** 10584–10589
15. Weber-Ban, E. U., Reid, B. G., Miranker, A. D., and Horwich, A. L. (1999) *Nature* **401,** 90–93
16. Hoskins, J. R., Singh, S. K., Maurizi, M. R., and Wickner, S. (2000) *Proc. Natl. Acad. Sci. U. S. A.* **97,** 8892–8897
17. Kim, Y. I., Burton, R. E., Burton, B. M., Sauer, R. T., and Baker, T. A. (2000) *Mol. Cell* **5,** 639–648
18. Singh, S. K., Grimaud, R., Hoskins, J. R., Wickner, S., and Maurizi, M. R. (2000) *Proc. Natl. Acad. Sci. U. S. A.* **97,** 8898–8903
19. Lee, C., Schwartz, M. P., Prakash, S., Iwakura, M., and Matouschek, A. (2001) *Mol. Cell* **7,** 627–637
20. Reid, B. G., Fenton, W. A., Horwich, A. L., and Weber-Ban, E. U. (2001) *Proc. Natl. Acad. Sci. U. S. A.* **98,** 3768–3772
21. Beinker, P., Schlee, S., Groemping, Y., Seidel, R., and Reinstein, J. (2002) *J. Biol. Chem.* **277,** 47160–47166
22. Clarke, A. K., and Eriksson, M. J. (2000) *J. Bacteriol.* **182,** 7092–7096
23. Barnett, M. E., Zolkiewska, A., and Zolkiewski, M. (2000) *J. Biol. Chem.* **275,** 37565–37571
24. Mogk, A., Schlieker, C., Strub, C., Rist, W., Weibezahn, J., and Bukau, B. (2003) *J. Biol. Chem.* **278,** 17615–17624
25. Lo, J. H., Baker, T. A., and Sauer, R. T. (2001) *Protein Sci.* **10,** 551–559
26. Singh, S. K., Rozycki, J., Ortega, J., Ishikawa, T., Lo, J., Steven, A. C., and Maurizi, M. R. (2001) *J. Biol. Chem.* **276,** 29420–29429
27. Flanagan, J. M., Wall, J. S., Capel, M. S., Schneider, D. K., and Shanklin, J. (1995) *Biochemistry* **34,** 10910–10917
28. Roberts, J. D., and McMacken, R. (1983) *Nucleic Acids Res.* **11,** 7435–7452
29. Baker, T. A., Mizuuchi, M., Savilahti, H., and Mizuuchi, K. (1993) *Cell* **74,** 723–733

30. Morgan, G. J., Hatfull, G. F., Casjens, S., and Hendrix, R. W. (2002) *J. Mol. Biol.* **317,** 337–359
31. Bohn, C., Binet, E., and Bouloc, P. (2002) *Mol. Genet. Genomics* **266,** 827–831
32. Bowie, J. U., and Sauer, R. T. (1989) *Biochemistry* **28,** 7139–7143
33. Norby, J. G. (1988) *Methods Enzymol.* **156,** 116–119
34. Banecki, B., Wawrzynow, A., Puzewicz, J., Georgopoulos, C., and Zylicz, M. (2001) *J. Biol. Chem.* **276,** 18843–18848
35. Mhammedi-Alaoui, A., Pato, M., Gama, M. J., and Toussaint, A. (1994) *Mol. Microbiol.* **11,** 1109–1116
36. Levchenko, I., Luo, L., and Baker, T. A. (1995) *Genes Dev.* **9,** 2399–2408
37. Kim, Y. I., Levchenko, I., Fraczkowska, K., Woodruff, R. V., Sauer, R. T., and Baker, T. A. (2001) *Nat. Struct. Biol.* **8,** 230–233
38. Wawrzynow, A., Wojtkowiak, D., Marszalek, J., Banecki, B., Jonsen, M., Graves, B., Georgopoulos, C., and Zylicz, M. (1995) *EMBO J.* **14,** 1867–1877
39. Burton, R. E., Siddiqui, S. M., Kim, Y. I., Baker, T. A., and Sauer, R. T. (2001) *EMBO J.* **20,** 3092–3100
40. Zeth, K., Ravelli, R. B., Paal, K., Cusack, S., Bukau, B., and Dougan, D. A. (2002) *Nat. Struct. Biol.* **9,** 906–911
41. Guo, F., Esser, L., Singh, S. K., Maurizi, M. R., and Xia, D. (2002) *J. Biol. Chem.* **277,** 46753–46762
42. Li, J., and Sha, B. (2003) *Structure* **11(3),** 323–328
43. Pace, C. N., and Shaw, K. L. (2000) *Proteins* **4,** (suppl.) 1–7